

Hindered proton collectivity in ${}^{28}_{16}\text{S}_{12}$: Possible magic number at $Z = 16$

Y. Togano,^{1,2,*} Y. Yamada,² N. Iwasa,³ K. Yamada,¹ T. Motobayashi,¹ N. Aoi,¹
H. Baba,¹ S. Bishop,¹ X. Cai,⁴ P. Doornenbal,¹ D. Fang,⁴ T. Furukawa,¹ K. Ieki,²
T. Kawabata,⁵ S. Kanno,¹ N. Kobayashi,⁶ Y. Kondo,¹ T. Kuboki,⁷ N. Kume,³
K. Kurita,² M. Kurokawa,¹ Y. G. Ma,⁴ Y. Matsuo,¹ H. Murakami,¹ M. Matsushita,²
T. Nakamura,⁶ K. Okada,² S. Ota,⁵ Y. Satou,⁶ S. Shimoura,⁵ R. Shioda,²
K. N. Tanaka,⁶ S. Takeuchi,¹ W. Tian,⁴ H. Wang,⁴ J. Wang,⁸ and K. Yoneda¹

¹*RIKEN Nishina Center, Saitama 351-0198, Japan*

²*Department of Physics, Rikkyo University, Tokyo 171-8501, Japan*

³*Department of Physics, Tohoku University, Miyagi 980-8578, Japan*

⁴*Shanghai Institute of Applied Physics,*

Chinese Academy of Science, Shanghai 201800, China

⁵*Center for Nuclear Study, University of Tokyo, Saitama 351-0198, Japan*

⁶*Department of Physics, Tokyo Institute of Technology, Tokyo 152-8551, Japan*

⁷*Department of Physics, Saitama University, Saitama 338-8570, Japan*

⁸*Institute of Modern Physics, Chinese Academy of Science, Lanzhou 730000, China*

(Dated: October 15, 2018)

Abstract

The reduced transition probability $B(\text{E}2; 0_{gs}^+ \rightarrow 2_1^+)$ for ${}^{28}\text{S}$ was obtained experimentally using Coulomb excitation at 53 MeV/nucleon. The resultant $B(\text{E}2)$ value $181(31) \text{ e}^2\text{fm}^4$ is smaller than the expectation based on empirical $B(\text{E}2)$ systematics. The double ratio $|M_n/M_p|/(N/Z)$ of the $0_{gs}^+ \rightarrow 2_1^+$ transition in ${}^{28}\text{S}$ was determined to be $1.9(2)$ by evaluating the M_n value from the known $B(\text{E}2)$ value of the mirror nucleus ${}^{28}\text{Mg}$, showing the hindrance of proton collectivity relative to that of neutrons. These results indicate the emergence of the magic number $Z = 16$ in the $|T_z| = 2$ nucleus ${}^{28}\text{S}$.

PACS numbers: 23.20.Js, 25.60.-t, 25.70.De

* Present address: EMMI, GSI, D-64291 Darmstadt, Germany

Magic numbers characterize the shell structure of fermionic quantum system such as atoms, metallic clusters [1] and nuclei [2]. A unique feature of the nuclear system is the fact that it comprises two types of fermions, the protons and neutrons, and hence the magic numbers appear both for protons and neutrons. Most of the recent studies regarding the magic numbers are for neutron-rich nuclei. Disappearance of the conventional magic numbers of $N=8, 20$ and 28 [3–5] or the appearance of the new magic number $N = 16$ [6–8] has been shown. They are associated with nuclear collectivity, which is enhanced, for instance, in the neutron-rich $N = 20$ nucleus ^{32}Mg caused by disappearance of the magic number [9, 10].

The new neutron magic number $N = 16$ has been confirmed experimentally for ^{27}Na ($|T_z| = 5/2$) and more neutron-rich isotones [6–8, 11, 12]. Its appearance can be theoretically interpreted as a result of a large gap between the neutron $d_{3/2}$ and $s_{1/2}$ orbitals caused by the low binding energy [6] and/or the spin-isospin dependent part of the residual nucleon-nucleon interaction [13]. In analogy to the magic number $N = 16$, the proton magic number $Z = 16$ must also exist in proton-rich nuclei. However, it has not been identified experimentally in the proton-rich sulfur isotopes. The present Letter reports on a study of the magic number $Z = 16$ at the most proton-rich even-even isotope ^{28}S with $|T_z| = 2$ through a measurement of the reduced transition probability $B(\text{E}2; 0_{gs}^+ \rightarrow 2_1^+)$.

The $B(\text{E}2)$ value is directly related to the amount of quadrupole collectivity of protons. The relative contribution of the proton- and neutron-collectivities can be evaluated using the ratio of the neutron transition matrix element to the proton one (the M_n/M_p ratio) for $0_{gs}^+ \rightarrow 2_1^+$ transitions [14, 15]. M_p is related to $B(\text{E}2)$ by $e^2 M_p^2 = B(\text{E}2; 0_{gs}^+ \rightarrow 2_1^+)$. The M_n value can be deduced from the M_p value in the mirror nucleus, where the numbers of protons and neutrons are interchanged. If collective motions of protons and neutrons have the same amplitudes, the double ratio $|M_n/M_p|/(N/Z)$ is, therefore, expected to be unity. Deviation from $|M_n/M_p|/(N/Z) = 1$ corresponds to a proton/neutron dominant excitation and should indicate a difference in the motions of protons and neutrons. Such a difference appears typically for the singly-magic nuclei [14, 16]. For proton singly-magic nuclei, the proton collectivity is hindered by the magicity, leading to $|M_n/M_p|/(N/Z) > 1$. For example, the singly-magic nucleus ^{20}O has a large double ratio of $1.7 \sim 2.2$ for the $0_{gs}^+ \rightarrow 2_1^+$ transition [17–19].

We used Coulomb excitation at an intermediate energy to extract the $B(\text{E}2; 0_{gs}^+ \rightarrow 2_1^+)$ value of the proton-rich nucleus ^{28}S . Intermediate-energy Coulomb excitation is a powerful

tool to obtain $B(E2)$ with relatively low intensity beams because a thick target is available [10, 20]. The double ratio $|M_n/M_p|/(N/Z)$ of the $0_{gs}^+ \rightarrow 2_1^+$ transition is obtained by combining the $B(E2)$ values of ^{28}S and the mirror nucleus ^{28}Mg .

The experiment was performed using the RIBF (Radioactive Isotope Beam Factory) accelerator complex operated by RIKEN Nishina Center and Center for Nuclear Study, University of Tokyo. A ^{28}S beam was produced via projectile fragmentation of a 115-MeV/nucleon ^{36}Ar beam from the $K = 540$ MeV RIKEN Ring Cyclotron incident on a 531 mg/cm² thick Be target. The secondary beam was obtained by the RIKEN Projectile-fragment separator (RIPS) [21] using an aluminum energy degrader with a thickness of 221 mg/cm² and a wedge angle of 1.46 mrad placed at the first dispersive focus. The momentum acceptance was set to be $\pm 1\%$. A RF deflector system [22] was placed at the second focal plane of RIPS to purify the ^{28}S in the beam with intense contaminants (mostly of ^{27}P , ^{26}Si and ^{24}Mg) that could not be removed only by the energy loss in the degrader. Particle identification for the secondary beam was performed event-by-event by measuring time of flight (TOF), energy loss (ΔE), and the magnetic rigidity of each nucleus. TOF was measured by using a RF signal from the cyclotron and a 0.1 mm thick plastic scintillator located 103 cm upstream of the third focal plane. ΔE was obtained by a 0.1 mm thick silicon detector placed 117 cm upstream of the third focal plane. The average ^{28}S beam intensity was 120 s⁻¹, which corresponded to approximately 1.9% of the total intensity of the secondary beam. The secondary target was a 348 mg/cm²-thick lead sheet which was set at the third focal plane. The average beam energy at the center of the lead target was 53 MeV/nucleon. Three sets of PPACs [23] were placed 155.6 cm, 125.6 cm, and 66.2 cm upstream of the secondary target, respectively, to obtain the beam trajectory on the secondary target.

An array of 160 NaI(Tl) scintillator crystals, DALI2 [24], was placed around the target to measure de-excitation γ rays from ejectiles. The measured full energy peak efficiency was 30 % at 0.662 MeV, in agreement with a Monte-Carlo simulation made by the GEANT4 code, and the energy resolution was 9.5 % (FWHM). The full-energy-peak efficiency for 1.5 MeV γ rays emitted from the ejectile with the velocity of $0.32c$ was evaluated to be 16% by the Monte-Carlo simulation.

The scattering angle, energy loss (ΔE), and total energy (E) of the ejectiles from the lead target were obtained by a detector telescope located 62 cm downstream of the target. It consisted of four layers of silicon detectors arranged in a 5×5 matrix without 4 detectors

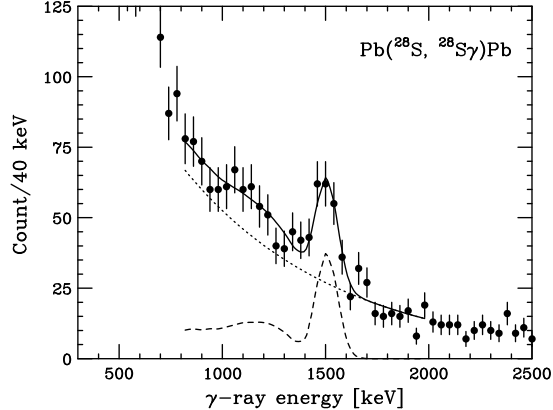


FIG. 1. Doppler-shift corrected γ -ray energy-spectrum in the $\text{Pb}(^{28}\text{S}, ^{28}\text{S}\gamma)\text{Pb}$ reaction. The fit by the response function (dashed curve) and the exponential background (dotted curve) is shown by the solid curve.

at the corners for the first two layers, and a 3×3 matrix for the third and fourth layers. The silicon detectors in the four layers had an effective area of $50 \times 50 \text{ mm}^2$ and a thickness of 500, 500, 325, and 500 μm , respectively. The detectors in the first and second layers had 5-mm-wide strip electrodes on one side to determine the hit position of the ejectiles. The ΔE - E method was employed to identify ^{28}S . The mass number resolution for sulfur isotopes was $0.35 (1\sigma)$. The angle of the ejectile was obtained from the hit position on the telescope and the beam angle and position on the target measured by the PPACs. The scattering angle resolution was 0.82 degree.

The Doppler-shift corrected γ -ray energy-spectrum measured in coincidence with inelastically scattered ^{28}S is shown in Fig. 1. A peak is clearly seen at 1.5 MeV. The spectrum was fitted by a detector response obtained by the Monte-Carlo simulation and an exponential background. The peak energy was obtained to be 1.497(11) MeV, which was consistent with the previous measurement, 1.512(8) MeV, by the two neutron removal reaction on ^{30}S [25]. This peak has been assigned to the transition from the 2_1^+ state to the 0^+ ground state [25]. In extracting the inelastic cross section, transitions feeding the 2_1^+ state were not accounted for, because the proton separation energy of 2.46(3) MeV is relatively low and no higher excited states were seen in the present spectrum and the two-neutron removal reaction on ^{30}S [25]. This was supported by the location of the second excited state in the mirror nucleus ^{28}Mg of 3.86 MeV.

The angular distribution of the scattered ^{28}S excited to its 1.5 MeV state is shown in

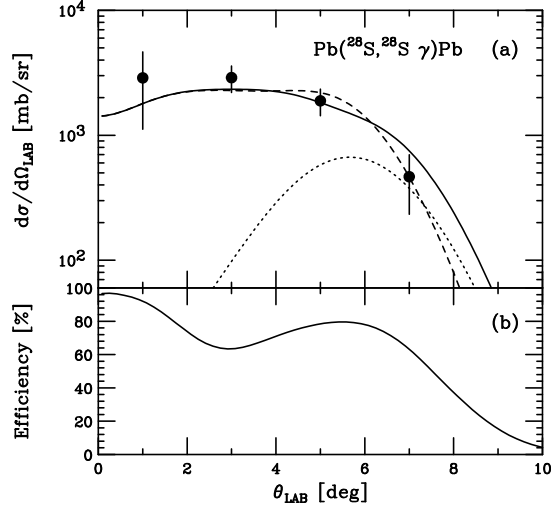


FIG. 2. (a) Angular distribution for the $\text{Pb}(^{28}\text{S}, ^{28}\text{S} \gamma)\text{Pb}$ reaction exciting the 1.5 MeV state in ^{28}S . The solid curve represents the best fit with ECIS calculation assuming $\Delta L = 2$. The dashed and dotted curves show the Coulomb and nuclear contributions, respectively. (b) Detection efficiency calculated by the Monte-Carlo simulation.

Fig. 2(a). Figure 2(b) shows the angle-dependence of the detection efficiency for scattered ^{28}S obtained by a Monte-Carlo simulation. It took into account the spacial and angular distributions of the ^{28}S beam, the size of the silicon detectors, and effect of multiple scattering in the target. The cross section integrated up to 8 degree was obtained to be 99(16) mb by taking into account the angle-dependent detection efficiency. The error was nearly all attributed to the statistical uncertainties, while the systematic errors of the γ -ray detection efficiency and the angle-dependence of the detection efficiency were also included (3%). The distribution was fitted by that for an angular momentum transfer of $\Delta L = 2$, calculated by the coupled-channel code ECIS97 [26] taking into account the scattering angle resolution. As seen in the figure, the $\Delta L = 2$ distribution well reproduced the experimental one, supporting the 2^+ assignment for the 1.5 MeV state. The ECIS calculation is almost equivalent to the distorted wave born approximation, since higher-order processes are negligible in the present experimental conditions. The optical potential parameters were taken from the study of the $^{17}\text{O} + ^{208}\text{Pb}$ elastic scattering at 84 MeV/nucleon [27]. The collective deformation model was employed to obtain a form factor for nuclear excitation. The Coulomb- and nuclear-deformation parameters β_C and β_N were employed to obtain the $B(E2)$ value as

$B(E2) = (3ZeR^2/4\pi)^2\beta_C^2$. β_N is related to β_C by a Bernstein prescription [14],

$$\frac{\beta_N}{\beta_C} = \frac{1 + (b_n^F/b_p^F)(M_n/M_p)}{1 + (b_n^F/b_p^F)(N/Z)}, \quad (1)$$

where $b_{n(p)}^F$ is the interaction strength of a probe F with neutrons (protons) in the nucleus. b_n^F/b_p^F is estimated to be 0.81 for the inelastic scattering on Pb at around 50 MeV/nucleon [19]. The M_n was deduced from the adopted $B(E2)$ value of the mirror nucleus ^{28}Mg [28]. The $B(E2)$ value for ^{28}S was obtained by adjusting β_C and hence M_p with β_N calculated by eq. (1) to reproduce the experimental angular distribution. The dashed and dotted curves in Fig. 2 shows the Coulomb and nuclear contributions, respectively. The use of the optical potential determined from the $^{40}\text{Ar} + ^{208}\text{Pb}$ scattering [29] gave a 5.5% smaller $B(E2)$ value. By taking the average of the results with the two optical potentials, the $B(E2;0_{gs}^+ \rightarrow 2_1^+)$ value was determined to be 181(31) e^2fm^4 . The associated error included the uncertainty of the measured cross section and the systematic error due to the choice of optical potentials. The $B(E2;0_{gs}^+ \rightarrow 2_1^+)$ value for the ^{24}Mg , a contaminant of the secondary beam, was obtained to be 444(66) e^2fm^4 by the same analysis. This agreed with the adopted value of 432(11) e^2fm^4 [28], exhibiting the reliability of the present analysis for ^{28}S .

The $B(E2)$ and $E_x(2_1^+)$ values for $Z = 16$ isotopes are plotted in Fig. 3(a) and (b), respectively. The filled circles show the present results. The open triangles for $B(E2)$ and $E_x(2_1^+)$ represent known values for the $Z = 16$ isotopes up to $A = 40$ [28]. The $B(E2)$ value increases from ^{36}S , the neutron singly-magic nucleus, to ^{30}S , and decreases at ^{28}S . On the other hand, the 2_1^+ energy of ^{28}S is smaller than those of $^{30-36}\text{S}$. These features contradict the empirical systematics. For example, Raman proposed the relation $B(E2) = (25.7 \pm 4.5)E_x(2_1^+)^{-1}Z^2A^{-2/3}$ which is obtained by a global fit to $E_x(2_1^+)$ and $B(E2)$ in a wide range of nuclei [28]. The shaded band in Fig. 3(a) represents the $B(E2)$ values calculated by this formula. As clearly seen, the present data for ^{28}S is much smaller than the expectation of 472(83) e^2fm^4 . An explanation of these small $B(E2)$ and $E_x(2_1^+)$ is given by the hindered proton collectivity and the neutron dominance in the $0_{gs}^+ \rightarrow 2_1^+$ transition. A similar mechanism is proposed for ^{16}C [31–33] and ^{136}Te [34, 35], where small $B(E2)$ and $E_x(2_1^+)$ values in comparison with neighboring isotopes are observed.

Figure 3(c) shows the double ratio $|M_n/M_p|/(N/Z)$ of the $Z = 16$ isotopes. The filled circle and open triangles show the present result and the known values, respectively. They are obtained by the $B(E2)$ values of the mirror pairs. The open squares represent the double

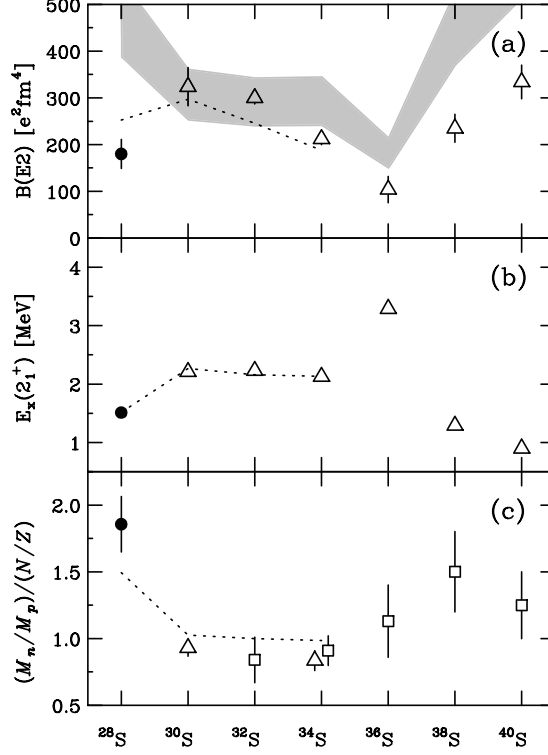


FIG. 3. Plot of the $B(E2;0_{gs}^+ \rightarrow 2_1^+)$ values (a), the excitation energies of 2_1^+ states (b), and the double ratio $|M_n/M_p|/(N/Z)$ (c) for sulfur ($Z = 16$) isotopes. The shell model predictions with the USDB interaction [30] are shown by the dotted curves for each quantity. The shaded region represents the $B(E2)$ predictions by the empirical $B(E2)$ systematics [28]. The present result is represented by the filled circles.

ratios obtained by the combinations of $B(E2)$ and the result of (p, p') on the nuclei of interest [36]. The ratio for ^{28}S amounts to 1.9(2) by taking the present result and adopted $B(E2)$ of 350(50) $e^2\text{fm}^4$ for the mirror nucleus ^{28}Mg [28]. The double ratio of 1.9(2) is significantly larger than unity indicating again the hindered proton collectivity relative to neutron and the neutron dominance in the $0_{gs}^+ \rightarrow 2_1^+$ transition in ^{28}S . This hindrance can be understood if ^{28}S is the proton singly-magic nucleus by the $Z = 16$ magicity. This picture is supported by the larger $B(E2)$ value and $|M_n/M_p|/(N/Z) \sim 1$ of the neighboring $N = 12$ isotones: 356 $e^2\text{fm}^4$ and 1.05(6) for ^{26}Si [28, 37], and 432(11) $e^2\text{fm}^4$ and 0.95(8) for ^{24}Mg [28, 38]. The double ratios of $^{30-36}\text{S}$ are close to unity, as seen in the figure, indicating that the hindrance of the proton collectivity does not appear in these nuclei. The large double ratios for $^{38,40}\text{S}$ can be explained by the neutron skin effect caused by the $Z = 16$ sub-shell closure [36, 39].

The dotted lines in Fig. 3 (a)-(c) show shell model predictions with the USDB effective interaction using the effective charges of $e_p = 1.36$ and $e_n = 0.45$ [30, 40]. The calculation shows excellent agreement with the experimental $E_x(2_1^+)$ values. The overall tendencies of the $B(E2)$ and $|M_n/M_p|/(N/Z)$ are reasonably reproduced. Especially the sudden decrease of $B(E2)$ and increase of $|M_n/M_p|/(N/Z)$ at ^{28}S are mostly predicted. It indicates that the shell model calculation with the USDB interaction accounts for the phenomena observed in the present study. It should be noted that the model interprets the $N = 16$ magicity in neutron-rich nuclei with the large $s_{1/2}$ - $d_{3/2}$ gap, and hence the $Z = 16$ magicity in proton-rich nuclei is inherent in the model reflecting the isospin symmetry. Slight difference remaining between the predictions and the experimental data may require further development of the theory.

In summary, the $B(E2; 0_{gs}^+ \rightarrow 2_1^+)$ value for the proton-rich nucleus ^{28}S was measured using Coulomb excitation at 53 MeV/nucleon. The resultant $B(E2)$ value is determined to be $181(31) \text{ e}^2\text{fm}^4$. The double ratio $|M_n/M_p|/(N/Z)$ for the $0_{gs}^+ \rightarrow 2_1^+$ transition in ^{28}S is obtained to be $1.9(2)$, by evaluating the M_n value from the known $B(E2)$ value of the mirror nucleus ^{28}Mg . These results show a hindered proton collectivity relative to that of neutrons in ^{28}S . It indicates the emergence of $Z = 16$ magicity in the $|T_z| = 2$ nucleus ^{28}S . The systematics of the $|M_n/M_p|/(N/Z)$ values for the $Z = 16$ isotopes indicates that the hindrance of proton collectivity in proton-rich region appears only at ^{28}S .

The authors thank the staff of RIKEN Nishina Center for their work of the beam operation during the experiment. One of the authors (Y.T.) is grateful for the support of the Special Postdoctoral Researcher Program at RIKEN and Research Center for Measurement in Advanced Science at Rikkyo University.

-
- [1] W. D. de Heer, Rev. Mod. Phys. **65**, 611 (1993).
 - [2] M. G. Mayer, Phys. Rev. **75**, 1969 (1949).
 - [3] H. Iwasaki *et al.*, Phys. Lett. B **481**, 7 (2000).
 - [4] E. K. Warburton, J. A. Becker, and B. A. Brown, Phys. Rev. C **41**, 1147 (1990).
 - [5] B. Bastin *et al.*, Phys. Rev. Lett. **99**, 022503 (2007).
 - [6] A. Ozawa, T. Kobayashi, T. Suzuki, K. Yoshida, and I. Tanihata, Phys. Rev. Lett. **84**, 5493

- (2000).
- [7] R. Kanungo *et al.*, Phys. Rev. Lett. **102**, 152501 (2009).
 - [8] C. R. Hoffman *et al.*, Phys. Lett. **B672**, 17 (2009).
 - [9] C. Détraz *et al.*, Phys. Rev. C **19**, 164 (1979).
 - [10] T. Motobayashi *et al.*, Phys. Lett. B **346**, 9 (1995).
 - [11] J. Gibelin *et al.*, Phys. Rev. C **75**, 057306 (2007).
 - [12] M. W. Cooper *et al.*, Phys. Rev. C **65**, 051302 (2002).
 - [13] T. Otsuka *et al.*, Phys. Rev. Lett. **87**, 082502 (2001).
 - [14] A. M. Bernstein, V. R. Brown, and V. A. Madsen, Phys. Lett. B **103**, 255 (1981).
 - [15] A. M. Bernstein, V. R. Brown, and V. A. Madsen, Phys. Rev. Lett. **42**, 425 (1979).
 - [16] M. A. Kennedy, P. D. Cottle, and K. W. Kemper, Phys. Rev. C **46**, 1811 (1992).
 - [17] J. K. Jewell *et al.*, Phys. Lett. B **454**, 181 (1999).
 - [18] E. Kahn *et al.*, Phys. Lett. B **490**, 45 (2000).
 - [19] N. Iwasa *et al.*, Phys. Rev. C **78**, 024306 (2008).
 - [20] T. Glasmacher, Annu. Rev. Nucl. Part. Sci. **48**, 1 (1998).
 - [21] T. Kubo *et al.*, Nucl. Instrum. Methods Phys. Res. B **70**, 309 (1992).
 - [22] K. Yamada, T. Motobayashi, and I. Tanihata, Nucl. Phys. A **746**, 156c (2004).
 - [23] H. Kumagai *et al.*, Nucl. Instr. and Meth. A **470**, 562 (2001).
 - [24] S. Takeuchi *et al.*, RIKEN Acc. Prog. Rep. **36**, 148 (2003).
 - [25] K. Yoneda *et al.*, Phys. Rev. C **74**, 021303 (2006).
 - [26] J. Reynal, Coupled channel code ECIS97, unpublished (1997).
 - [27] J. Barrette *et al.*, Phys. Lett. B **209**, 182 (1988).
 - [28] S. Raman, C. W. Nestor JR, and P. Tikkanen, At. Data Nucl. Data. Tables **78**, 1 (2001).
 - [29] N. Alamanos *et al.*, Phys. Lett. B **137**, 37 (1984).
 - [30] B. A. Brown and W. A. Richter, Phys. Rev. C **74**, 034315 (2006).
 - [31] Z. Elekes *et al.*, Phys. Lett. B **586**, 34 (2004).
 - [32] H. J. Ong *et al.*, Phys. Rev. C **78**, 014308 (2008).
 - [33] M. Wiedeking *et al.*, Phys. Rev. Lett. **100**, 152501 (2008).
 - [34] D. C. Radford *et al.*, Phys. Rev. Lett. **88**, 222501 (2002).
 - [35] J. Terasaki, J. Engel, W. Nazarewicz, and M. Stoitsov, Phys. Rev. C **66**, 054313 (2002).
 - [36] F. Maréchal *et al.*, Phys. Rev. C **60**, 034615 (1999).

- [37] P. D. Cottle *et al.*, Phys. Rev. C **64**, 057304 (2001).
- [38] B. Zwieglinski, G. M. Crawley, H. Nann, and J. A. Nolen Jr., Phys. Rev. C **17**, 872 (1978).
- [39] N. Alamanos, F. Auger, B. A. Brown, and A. Pakou, J. Phys. G **24**, 1541 (1998).
- [40] W. A. Richter, S. Mkhize, and B. A. Brown, Phys. Rev. C **78**, 064302 (2008).